

# ZIRAT-11 SPECIAL TOPIC REPORT

## **Pellet-Cladding Interaction (*PCI* and *PCMI*)**

*Authors*

**Ron Adamson**

Zircology Plus, Fremont, California, USA

**Brian Cox**

University of Toronto, Ontario, Canada

**John Davies**

San Jose, California, USA

**Friedrich Garzarolli**

Erlangen, Germany

**Peter Rudling**

ANT International, Skultuna, Sweden

**Sam Vaidyanathan**

San Jose, California, USA

*Edited by*

**Ron Adamson**

Zircology Plus, Fremont, California, USA

**October, 2006**

Advanced Nuclear Technology International  
Krongjutarvägen 2C, SE-730 50 SKULTUNA  
Sweden

[info@antinternational.com](mailto:info@antinternational.com)



[www.antinternational.com](http://www.antinternational.com)

## DISCLAIMER

The information presented in this report has been compiled and analysed by Advanced Nuclear Technology International Europe AB (*ANT* International) and its subcontractors. *ANT* International has exercised due diligence in this work, but does not warrant the accuracy or completeness of the information. *ANT* International does not assume any responsibility for any consequences as a result of the use of the information for any party, except a warranty for reasonable technical skill, which is limited to the amount paid for this assignment by each *ZIRAT* program member.

## FOREWORD

At the end of this report a conversion table appears providing conversion factors between SI and US units.

The personal viewpoints and conclusions presented in the report that are beyond those quoted from references are those of the individual authors and may not represent the collective view of all authors.

*Ron Adamson, Editor*

## ACRONYMS AND EXPLANATIONS

ADOPT	Advanced Doped Pellet Technology
AECL	Atomic Energy of Canada Limited
ALTA	Additive Lead Test Assemblies
ANT	Advanced Nuclear Technology
APSR	Axial Power Shaping Rods
BWR	Boiling Water Reactor
CANDU	CANada Deuterium Uranium
CEA	Commissariat à l'Energie Atomique
CEB	Closed-End Burst Test
CERT	Constant Extension RaTe
CILC	Crud Induced Localized Corrosion
CREA	Control Rod Ejection Accident
CRDA	Control Rod Drop Accident
CSED	Critical Strain Energy Density
CWSR	Cold Work and Stress Relieved
CZP	Cold Zero Power
DCB	Double Cantilever Beam
DN	Delayed Neutron
DNB	Departure from Nucleate Boiling
DP	Douglas Point
EBT	Equal Biaxial Tension
EDC	Expansion Due to Compression
EDM	Electric Discharge Machining
EM	Expanding Mandrel
EOC	End of Cycle
EOL	End Of Life
FGR	Fission Gas Release
FSAR	Final Safety Analysis Report
GE	General Electric
GETR	General Electric Test Reactor
GNF	Global Nuclear Fuel
HB	High Burnup
HGC	Hydrogen Gas Cracking
HPUF	Hydrogen PickUp Fraction
HZP	Hot Zero Power
IAEA	International Atomic Energy Agency
I.D.	Inner Diameter
IFA	Instrumented Fuel Assemblies
IG	InterGranular
IPT	Internally Pressurized Tubes
ISCC	Intergranular Stress Corrosion Cracking
JMTR	Japan Materials Test Reactor
KKL	KernKraftwerk Leibstadt

KWO	KernKraftwek Obrigheim
KWU	KraftWerkUnion
LDA	Localized Ductility Arc
LHGR	Linear Heat Generation Rate
LK	Låg corrosion (Low Corrosion in Swedish)
LME	Liquide Metal Embrittlement
LOCA	Loss of Coolant Accident
LTA	Lead Test Assemblies
LUA	Lead Use Assemblies
LWR	Light Water Reactor
MDA	Mitsubishi Developed Alloy
MOX	Mixed OXide
MVE	Metal-Vapour Embrittlement
NDA	New Developed Alloy
NFIR	Nuclear Fuel Industry Research
NGS	Nuclear Generting Station
NPD	Nuclear Power Demonstration
NRC	Nuclear Regulatory Commission
NSRR	Nuclear Safety Research Reactor
NUPEC	NUclear Power Engineering Corporation
O.D.	Outer Diameter
OEB	Open-End Burst
OIC	Outside-In-Cracking
PCI	Pellet Cladding Interaction
PCIOMR	Pellet Cladding Interaction Operating Management Restrictions
PCMI	Pellet Cladding Mechanical Interaction
PGS	Pickering Generation Station
PIE	Post-Irradiation Examinations
PWR	Pressurised Water Reactor
RA	Reduction in Area
RH	Ramp and Hold
RIA	Reactivity Initiated Accident
RT	Room Temperature
RX	Recrystallised
RXA	Recrystallised Annealed
SCC	Stress Corrosion Cracking
SED	Strain-Energy Density
SEM	Scanning Electron Microscopy
SIMFEX	SIMulated Fuel EXpansion
SRP	Standard Review Plan
SRP	Segmented Rod Program
SS	Stainless Steel
STR	Special Topic Report
SRA	Stress Relieved Annealed
TAT	Tube Axial Tension

## ZIRAT-11 Special Topic on Pellet Cladding Interaction

TD	Theoretical Density
TE	Total Elongation
TEM	Transmission Electron Microscopy
TFGR	Transient Fission Gas Release
TG	TransGranular
TSS	Terminal Solid Solubility
UE	Uniform Elongation
US	Ultimate Strength
UTS	Ultimate Tensile Strength
UTT	Uniaxial Tensile Test
ZIRLO	ZIRconium Low Oxidation

## UNIT CONVERSION

TEMPERATURE		
$^{\circ}\text{C} + 273,15 = \text{K}$		
$^{\circ}\text{C} * 1,8 + 32 = ^{\circ}\text{F}$		
T(K)	T (°C)	T(°F)
273	<b>0</b>	32
289	16	61
298	25	<b>77</b>
373	<b>100</b>	212
473	<b>200</b>	392
573	<b>300</b>	572
633	360	680
673	<b>400</b>	<b>752</b>
773	<b>500</b>	932
783	510	950
793	520	968
823	550	1022
833	560	1040
873	<b>600</b>	1112
878	605	1121
893	620	1148
923	650	1202
973	<b>700</b>	1292
1023	750	1382
1053	780	1436
1073	<b>800</b>	1472
1136	863	1585
1143	870	1598
1173	<b>900</b>	1652
1273	<b>1000</b>	1832
1343	1070	1958
1478	1204	<b>2200</b>

MASS	
kg	lbs
0,454	<b>1</b>
<b>1</b>	2,20

DISTANCE	
x (μm)	x (mils)
0,6	0,02
<b>1</b>	0,04
5	0,20
<b>10</b>	0,39
20	0,79
25	0,98
25,4	<b>1,00</b>
<b>100</b>	3,94

PRESSURE		
bar	MPa	psi
<b>1</b>	0,1	14
10	<b>1</b>	142
<b>70</b>	<b>7</b>	995
70,4	7,04	<b>1000</b>
<b>100</b>	10	1421
130	13	<b>1847</b>
155	15,5	2203
<b>704</b>	<b>70,4</b>	<b>10000</b>
<b>1000</b>	100	14211

STRESS INTENSITY FACTOR	
MPa√m	ksi√inch
0,91	<b>1</b>
<b>1</b>	1,10



## CONTENTS

## ACRONYMS AND EXPLANATIONS

V

## UNIT CONVERSION

VIII

<b>1</b>	<b>PCI AND PCMI - AN INTRODUCTION (PETER RUDLING)</b>	<b>1-11</b>
1.1	PARAMETERS IMPACTING PCI/PCMI	1-26
1.1.1	Time	1-26
1.1.2	Aggressive environment	1-28
1.1.3	Cladding loading conditions	1-29
1.1.3.1	Stress state	1-29
1.1.3.2	Strain rate	1-31
1.1.3.3	Stress	1-34
1.1.3.3.1	Effect of barrier/liner/lubricants	1-34
1.1.3.3.2	Pellet design and defects	1-36
1.1.3.3.3	Fuel assembly design	1-46
1.1.3.3.4	Operation restrictions	1-46
1.1.4	Cladding Embrittlement	1-53
1.1.4.1	Irradiation damage	1-53
1.1.4.2	Oxide layer	1-53
1.1.4.3	Hydrides	1-54
1.1.5	Cladding microstructure	1-55
1.1.6	Bump	1-56
1.1.7	Transient Fission Gas-Release, <i>TFGR</i>	1-60
<b>2</b>	<b>PCI DETAILS AND MODELS</b>	<b>2-1</b>
2.1	PCI PHENOMENA	2-1
2.1.1	General models and features (Ron Adamson)	2-1
2.1.2	Test methods (Ron Adamson)	2-12
2.1.2.1	In-reactor ramp tests	2-12
2.1.2.2	Laboratory tests	2-14
2.1.2.2.1	Testing criteria	2-14
2.1.2.2.1.1	Simulate <i>PCI</i> conditions	2-14
2.1.2.2.1.2	Avoid extraneous chemistry effects	2-16
2.1.2.2.2	Test techniques	2-17
2.1.2.2.3	Important test results	2-24
2.1.2.2.3.1	Effect of environment	2-24
2.1.2.2.3.2	Effect of strain rate	2-27
2.1.2.2.3.3	Effects of irradiation	2-28
2.1.2.2.3.4	Effects of inner surface liners	2-31
2.1.2.2.4	References related to specific topics	2-33
2.1.3	Mechanisms (Brian Cox)	2-35
2.1.3.1	Introduction	2-35
2.1.3.2	Mechanistic Deductions from the early <i>PCI</i> failures	2-41
2.1.3.3	Other Mechanistic Factors	2-49
2.1.3.4	Correlation of Laboratory and In-Reactor Observations	2-53
2.1.3.5	SCC and <i>PCI</i> Fractography	2-55
2.1.3.6	A <i>PCI</i> Mechanism that fits the observations	2-57
2.2	REMEDIES	2-60
2.2.1	Cladding liners (Friedrich Garzarolli)	2-60
2.2.1.1	Development of the Zr Liner by GE (today GNF)	2-60
2.2.1.2	Operation Experience with Zr Liner-Fuel in BWRs.	2-65
2.2.1.3	Post Defect Behaviour of Zr Liner-Fuel in BWRs	2-65
2.2.1.4	Development of the Zr-Sn Liner by ABB (today Westinghouse)	2-69

## ZIRAT-11 Special Topic on Pellet Cladding Interaction

2.2.1.5	Development of the Zr-Fe Liner by Siemens (today AREVA NP)	2-72
2.2.1.6	Conclusion on Zr Liner	2-74
2.2.2	Fuel lubricants (Brian Cox)	2-77
2.2.3	Fuel additives (John Davies and Sam Vaidyanathan)	2-83
2.2.3.1	Introduction	2-83
2.2.3.2	Aluminosilicate grain-boundary phase additives	2-84
2.2.3.2.1	PCI Resistance	2-86
2.2.3.2.2	Fabrication and Properties	2-89
2.2.3.2.3	Fission gas-release and swelling behaviour	2-93
2.2.3.2.4	Irradiation experience	2-97
2.2.3.3	Cation dopants	2-99
2.2.3.3.1	Fission-gas release and creep	2-102
2.2.3.3.2	PCI Resistance of niobia ( $\text{Nb}_2\text{O}_5$ ) doped fuel	2-105
2.2.3.3.3	PCI Resistance of chromia ( $\text{Cr}_2\text{O}_3$ ) doped fuel	2-106
2.2.3.4	Discussion	2-110
<b>3</b>	<b>PELLET-CLADDING MECHANICAL INTERACTION (PCMI)</b> <b>(RON ADAMSON)</b>	<b>3-1</b>
3.1	EFFECTS OF HYDRIDES	3-1
3.2	REACTIVITY INSERTION ACCIDENT (RIA)	3-15
3.2.1	Mechanical Testing Techniques	3-17
3.2.1.1	Specimen Designs	3-18
3.2.2	Laboratory Test Data	3-26
3.2.2.1	Temperature	3-26
3.2.2.2	Temperature/Hydrides	3-26
3.2.2.3	Strain Rate	3-29
3.2.2.4	Irradiation	3-30
3.2.2.5	Mechanical Property Database	3-31
3.2.2.5.1	Older Data	3-31
3.2.2.5.2	Newer Data	3-32
3.2.2.6	Simulation Attempts	3-36
3.2.3	New Proposed Failure Criteria	3-40
3.2.3.1	Failure Criteria Summary	3-50
3.3	OUTSIDE-TO-INSIDE CRACKING (OTIC)	3-51
3.3.1	Hydride Rim Effects	3-51
3.3.2	Radial Hydride Effects	3-53
<b>4</b>	<b>SUMMARY</b>	<b>4-1</b>
4.1	OVERALL – SECTION 1	4-1
4.2	PCI PHENOMENA – SECTION 2.1	4-2
4.3	PCI REMEDIES – SECTION 2.2	4-5
4.4	EFFECTS OF HYDRIDES – SECTION 3.1	4-7
4.5	REACTIVITY INSERTION ACCIDENTS (RIA) – SECTION 3.2	4-8
4.6	OUTSIDE-IN CRACKING (OTIC) – SECTION 3.3	4-9
<b>5</b>	<b>REFERENCES</b>	<b>5-1</b>

## 1 *PCI AND PCMI - AN INTRODUCTION (PETER RUDLING)*

**Pellet Cladding Interaction, *PCI***, is associated with local power ramps during reactor startup or manoeuvring (e.g., rod adjustments/swaps, load following), Figure 1-1, and occurs under the influence of I, Cs and Cd in a susceptible material that may result in Stress Corrosion Cracking, *SCC*, of the fuel cladding, Figure 1-2. The crack always starts at the cladding inner surface and progresses towards the outer cladding diameter in the minute scale, Figure 1-3 and, Figure 1-4. The *PCI* failure mechanism is described in Section 2.1.3.

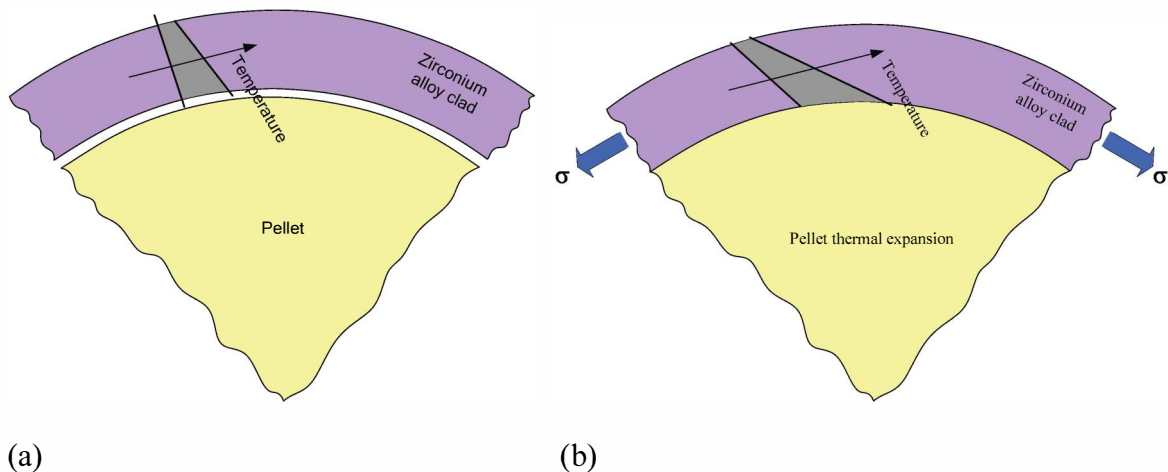


Figure 1-1: Schematics showing the fuel rod condition, (a) before the ramp and, (b) during the ramp.



Figure 1-2: Schematics showing the three components involved in *SCC*.

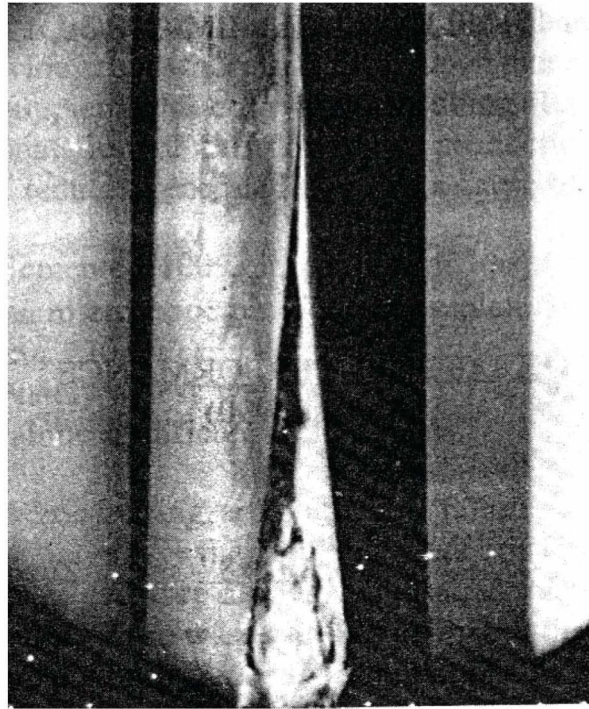


Figure 1-3: From Baily et al., 1991.

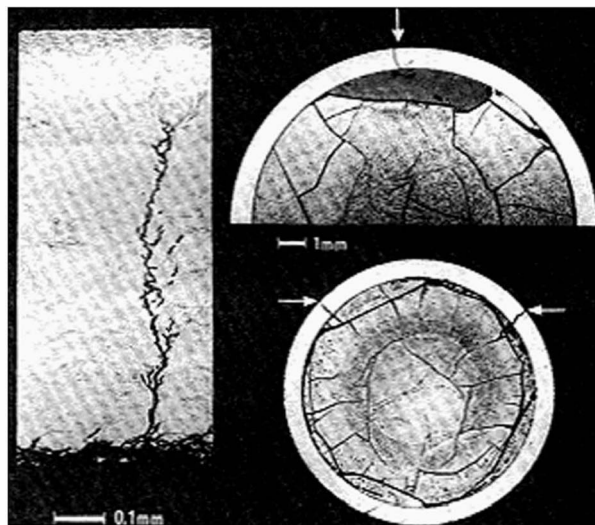


Figure 1-4: PCI Failures, Garzarolli et al., 1979.

*PCI* failures may occur in both pressurized water reactors (*PWRs*) and boiling water reactors (*BWRs*). The failure mechanism is much more prevalent in *BWRs* since reactor operation to some extent is done by control rods movements<sup>1</sup>. In *PWRs*, reactor power is normally not controlled by insertion and extraction of the control rods in the core; Instead, reactor power is controlled by the boron concentration that is continuously decreased during operation to compensate for the decrease in reactivity. This type of reactor power control is much smoother than in the *BWR* case and consequently *PCI* failures are less common in *PWRs*. However, during reactor power increases, and specifically during a class II transient (anticipated operational occurrence), *PCI* failures may occur in a *PWR*.

The first *PCI* failures were reported by Weidenbaum, 1961-1964. The failures occurred in a test program to assess how much fuel centre melting could be tolerated in a fuel rod during operation without leading to fuel-rod failure. Four different fuel assemblies were tested with successively increased surface heat flux during four different periods of time: 188-251-314-380 W/cm<sup>2</sup>. Each assembly contained four Zr-2 fuel rods with a cladding *O.D.* of 14.1 mm, a cladding thickness of 0.75 mm and a cold pellet-cladding gap of 150 µm. Metallographic cross sections of the fuel rods showed that fuel centre melting occurred at a surface heat flux exceeding 198 W/cm<sup>2</sup>. Weidenbaum could show that the cladding plastic strains were a result of the fuel volume expansion due to the fuel melting. During the irradiation of the test assembly *EPT-12*, three fuel rods failed and subsequent hot-cell examinations indicated that these failures as well as the failed rod in the previous test assembly *EPT-10* was iodine assisted stress corrosion cracking, *SCC*. This was the first time this failure mechanism had been noted, which subsequently became named as *PCI*. The examinations also revealed that the claddings diametral failure strains were very small, ranging from 1.7 to 3.3% in the failed *EPT-12* failures. Additional tests in *GETR* showed that fuel rods with cladding diameter strains smaller than 0.3% were intact.

Subsequent to the failures in the *GETR*, similar failures occurred in the Halden Boiling Water Reactor, Garlick, 1968, the U-1, U-2 and X-loops at Chalk River (*CANDU* reactor) as well as in the *CANDU* Douglas Point, *DP*, Reactor, Garlick, 1969. *PCI* failures also occurred following bundle refuelling movements in the Pickering Generation Station, *PGS*, *CANDU* reactor, Cox, 1990(b).

*PCI* failures in *BWRs* were identified as problem in 1971 following control blade movements, Williamson & Proebstle, 1975. Specifically, during the 1970s and 1980s, *PCI* was one of the major fuel failure causes in *BWRs* for fuel with burnup ranging from 5 to 25 MWd/kgU, Table 1-1.

<sup>1</sup> The reactor power in both *BWRs* and *PWRs* is also regulated by flow control.

Table 1-1: GE 8×8 Fuel Failure Experience up to August 1993 (number of failed assemblies), Potts & Probestle, 1994.

	1980	1981	1982	1983	1984	1985	1986	1987	1988	1989	1990	1991	1992	1993
<b>PCI</b>														
Non-barrier	8	4	4	12	9	4	16	7	13	1	2	0	0	2
Barrier	---	0	0	0	0	0	0	0	0	0	0	0	0	
<b>CILC</b>														
Conventional	7	67	55	47	79	41	22	16	42	13	4	1	0	0
Corrosion	---	---	---	---	0	0	0	0	0	45 <sup>a</sup>	0	0	0	0
Improved														
Debris fretting	2	1	2	2	2	0	1	0	3	0	2	13	4	2
Manufacturing defects	1	0	0	1	2	0	2	1	6	10	7	6	7	2
Unknown											1			6
<b>Total</b>	<b>18</b>	<b>72</b>	<b>61</b>	<b>62</b>	<b>92</b>	<b>45</b>	<b>41</b>	<b>24</b>	<b>64</b>	<b>69</b>	<b>16</b>	<b>20</b>	<b>11</b>	<b>12</b>

<sup>a</sup> Severe chemical intrusion event at one US reactor.



Figure 1-5 shows the large power increase in a fuel rod adjacent to a control rod that is pulled out of the core. The increase in rod power (Linear Heat Generation Rate, *LHGR*) will increase fuel temperature, which in turn will result in a thermal pellet expansion. If the pellet-cladding gap is small enough prior to the control rod pull, the pellet expansion will consume the initial pellet-cladding gap and result in cladding tensile stresses if the rod power increase is large enough. If the cladding stresses become large enough they may result in *PCI* fuel failures. Figure 1-6 shows the fuel rods that will experience the largest power increase during the extraction of the control rods. Thus, if a fuel failure occurs in a rod adjacent to the control rod that is pulled out of the core, the primary failure cause is most likely *PCI*. This may be an important piece of information since it is often hard to assess if the rod has failed due to *PCI* or not in hot-cell examinations since the failed rod may experience significant degradation. If *PCI* failure is a suspected failure cause, it is recommended that a symmetry rod to the failed rod is also sent to the hot cell. If the failure cause is *PCI*, *PCI* cracks will most likely also show up in the unfailed symmetry rod but in this case the *PCI* cracks will not have penetrated the whole cladding thickness.

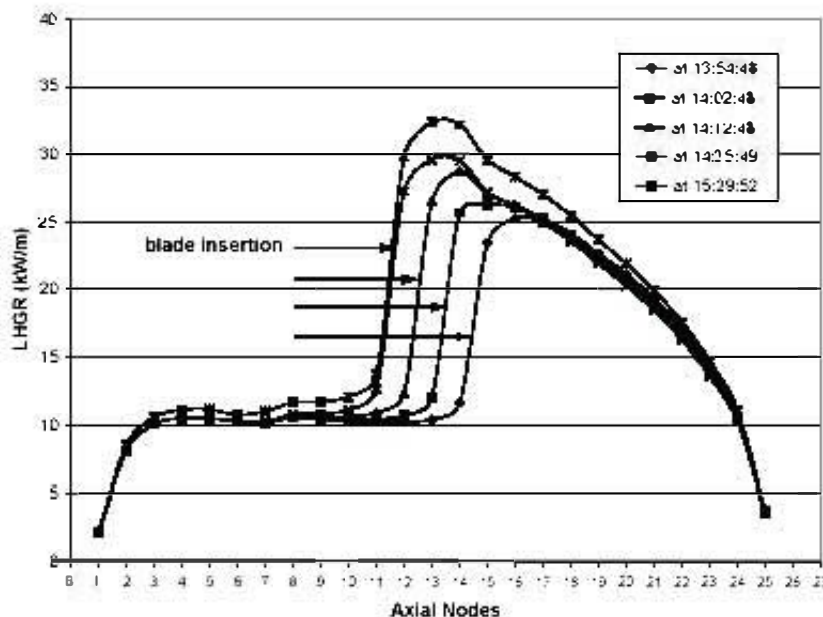


Figure 1-5: Effect of three successive 2-notch control blade pulls followed by return to full power on the axial power distribution, Billaux & Moon, 2004.

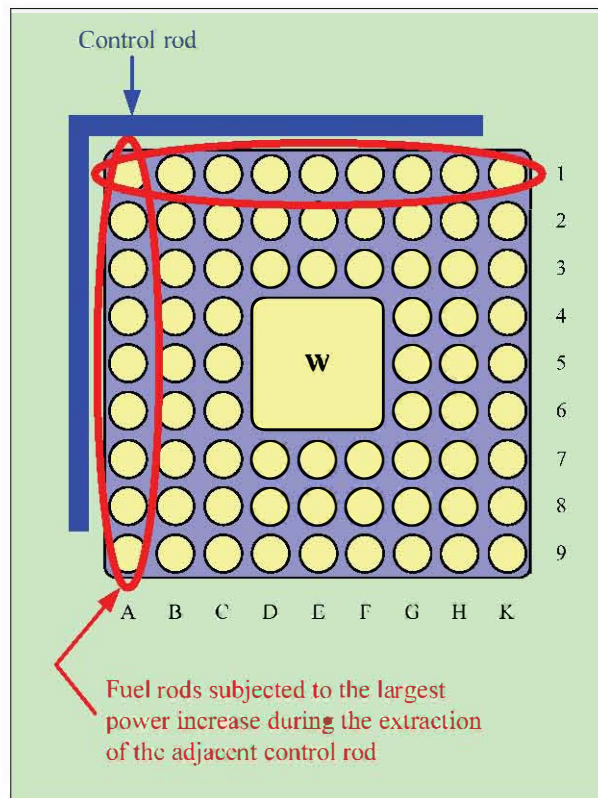


Figure 1-6: Figure showing the fuel rods that will be subjected to the largest power increase as the adjacent control rod is pulled out of the core.

During cycle 5 and 6 of the *KWU* designed Obrigheim *PWR* plant several *PCI* failures occurred due to power ramps early in the cycle, Figure 1-7. The *PCI* failures occurred at the lower rod elevation that experienced the largest power increase while secondary defect were formed in the upper part of the rods.



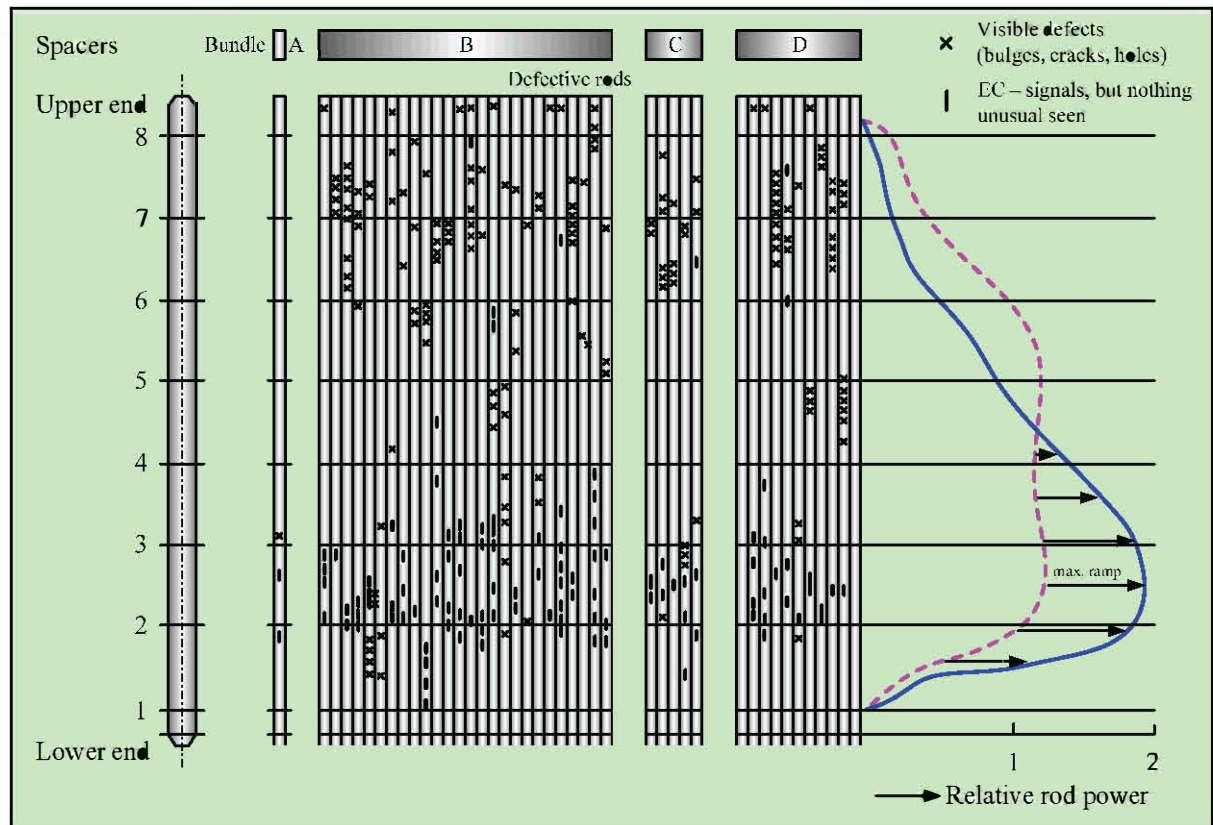


Figure 1-7: Correlation between power ramp and the location of defects (KW cycle 6), modified figure according to Garzarolli et al., 1978.

To prevent *PCI* failure, it is necessary to remove at least one of the fundamental conditions (tensile stress, sensitive material, aggressive environment), which cause *SCC*. There are two principal types of remedies.

- 1) One is to develop reactor operation restrictions that will ensure that the cladding stresses will always be below the *PCI* threshold stress during power increases. This is the main measure to avoid *PCI* defects and the only measure used in *PWRs*. Operating rules (also called management recommendations, or *PCIMRs*) to limit local power increases and “condition” fuel to power ramping were implemented during the late 70s to resolve the *PCI* issue. The rules are usually a function of exposure, and were developed by the different fuel vendors, so they differ between various fuel types, see Section 1.1.3.3.4. To establish and validate these rules, extensive power ramp tests were performed by the fuel vendors in experimental reactors.

However, these reactor operation restrictions result in significant reductions in the capacity factors in *BWRs*, whereas *PWRs* never suffered such large capacity losses, Figure 1-8.

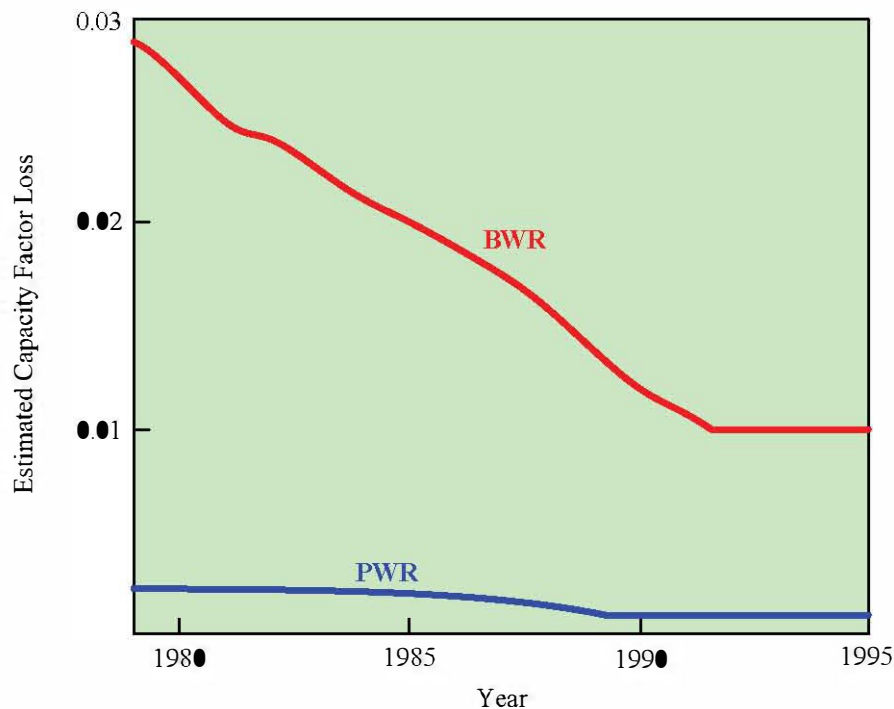


Figure 1-8: Estimated capacity loss from power manoeuvring restrictions related to *PCI*, modified figure according to Franklin, 1981.

2) The second remedy — design improvement — consists of several approaches.

a) Cladding design

- i) Development of radial cladding texture and small grain size may increase cladding *PCI* resistance, Garzarolli, 2001.
- ii) In the 1980s, GE developed the barrier/liner concept, initially with “pure” Zr metal barrier at the cladding *I.D.* that would reduce the cladding stresses, see Sections 1.1.3.3.1 and 2.2.1. Later fuel vendors realised that the Zr must be alloyed with Fe to improve the secondary degradation resistance if the rod should fail. The Fe in the Zr will dramatically improve the corrosion resistance of the liner/barrier but may reduce the *PCI* performance. The most representative one is the use of a zirconium barrier (liner) at the inner cladding surface. The barrier is soft and serves to reduce the local stress and hence to give cladding resistance to *SCC*. Although this remedy has so far only been used in *BWRs*, it should be equally applicable to *PWRs*.

b) Pellet design

- i) In the early 1970s it was found that *PCI* performance could be improved by reducing the cladding local strains by shortening the pellet, chamfering the corners and eliminating the dishing<sup>2</sup>, see Section 1.1.3.3.2.
- ii) “Soft” pellets are being developed both for *BWRs* and *PWRs*, that will reduce *PCI/PCMI* loading during the power ramp and thereby reduced the risk of *PCI/PCMI* failures, see Section 2.2.3. If the pellet is “soft” enough and the cladding strength is large enough, the cladding will contain the thermal pellet volume expansion (during the power ramp) and result in plastic creep deformation of the fuel pellet.

c) Fuel assembly design

- i) The modern *BWR* fuel assembly designs contain more fuel rods (by going from 7x7 -> 8x8 -> 9x9 -> 10x10 lattice designs) and therefore have a lower linear heat rating for each rod. In this way the fuel may permanently operate below the *PCI* threshold. However, the increased margins towards *PCI* have been used up by the utilities today, and the limiting fuel rods in the modern fuel assemblies (e.g., 10x10 fuel) now have about the same linear heat rating as the old fuel designs (e.g., 8x8 fuel).

Due to removal of some of the operating restrictions on *BWR* liner fuel, occurrence of pellet manufacturing defects and, more aggressive core loading patterns in *US BWRs* and *PWRs*, *PCI* failures have reoccurred, Figure 1-9 and Figure 1-10. It is noteworthy that some *PCI*-suspect failures were experienced in three B&W-designed *US PWR* plants following the movement of axial power shaping rods (*APSRs*) even though the calculated stress levels remained within the permissible range.

---

<sup>2</sup> Page: 19

However, the original reference for reduced cladding strains by changing pellet geometry (T.J. Carter, Nuclear Technology, 45 (1979) 166-176) also reported no improvement in *PCI* failures.

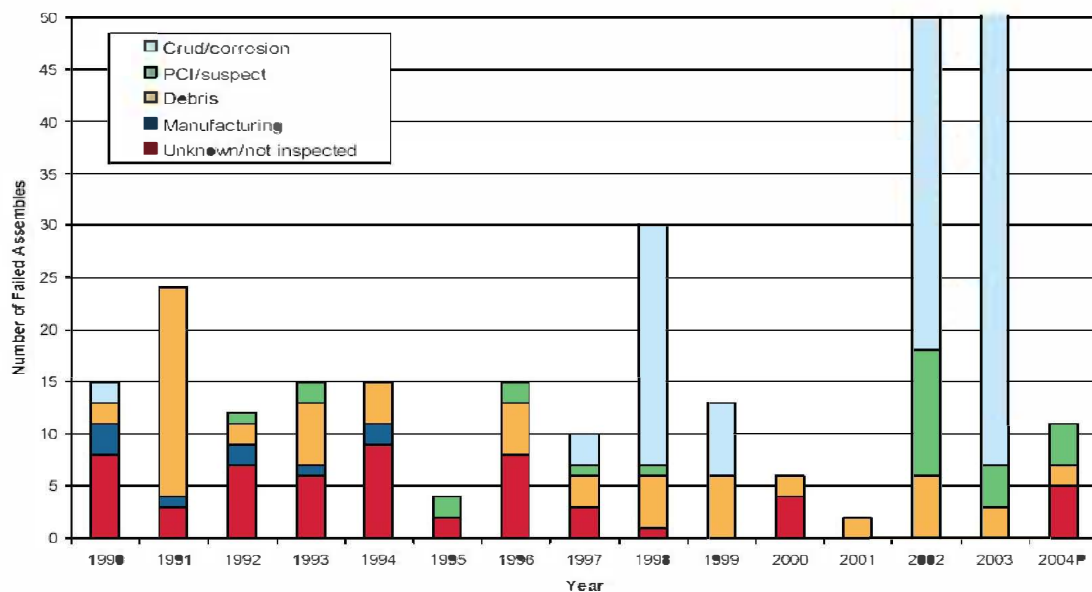


Figure 1-9: Trend in *US BWR* failure root causes (2004 results are incomplete), Yang et al., 2004.

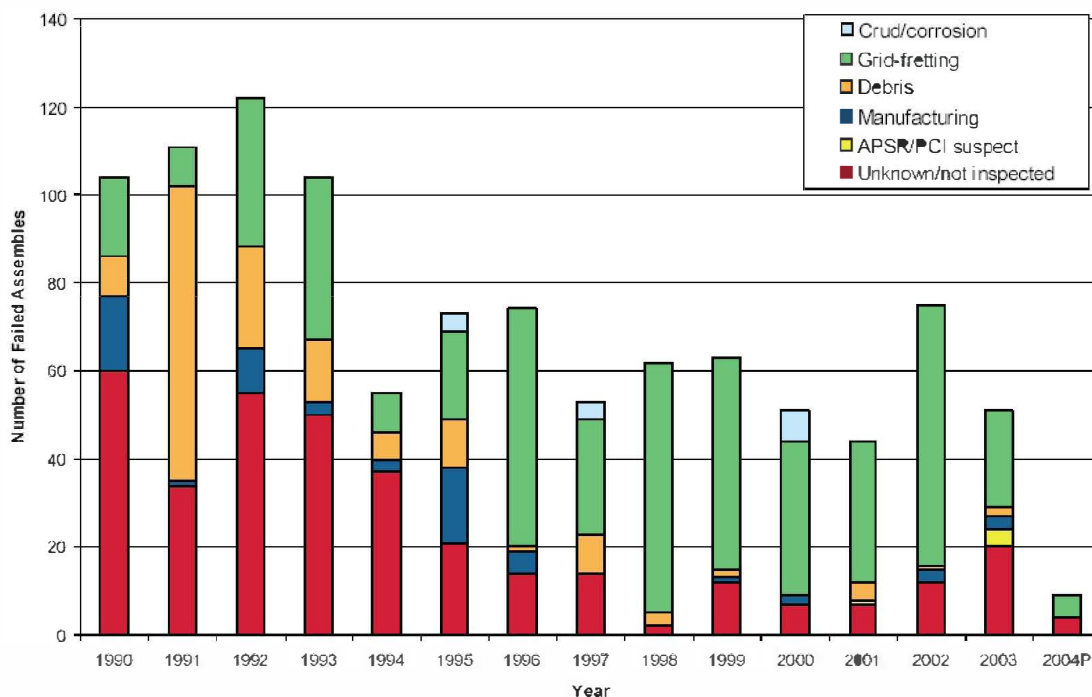


Figure 1-10: Trend in *US PWR* failure root causes (2004 results are incomplete), Yang et al., 2004.

Pellet-cladding mechanical interaction, *PCMI*, is a situation where the pellet and cladding interacts mechanically to the point that the cladding will break but without the impact of an *SCC* agent such as iodine. The stress is generated from a power increase resulting in an expanding pellet due to thermal expansion and in some cases fission-gas swelling. If these stresses become large enough, *PCMI* failures may occur.

A range of power-increasing transients where *PCMI* may be important are addressed in the Final Safety Analysis Report, *FSAR*, and reload licensing analyses (e.g., loss of feedwater heating in a *BWR* and steamline break in a *PWR*). If the *PCMI* stress is low enough or if the cladding ductility is high enough, *PCMI* failures will not occur. However, in these cases, the cladding temperature may increase to such an extent that the critical heat flux may be exceeded and lead to clad failures due to post-*dnb* (departure from nucleate boiling) failures (related to rewetting of the heavily oxidized and embrittled fuel cladding). As the burnup increases, the risk of post-*dnb* fuel failures decreases while the risk of failure due to *PCMI* increases, Figure 1-11

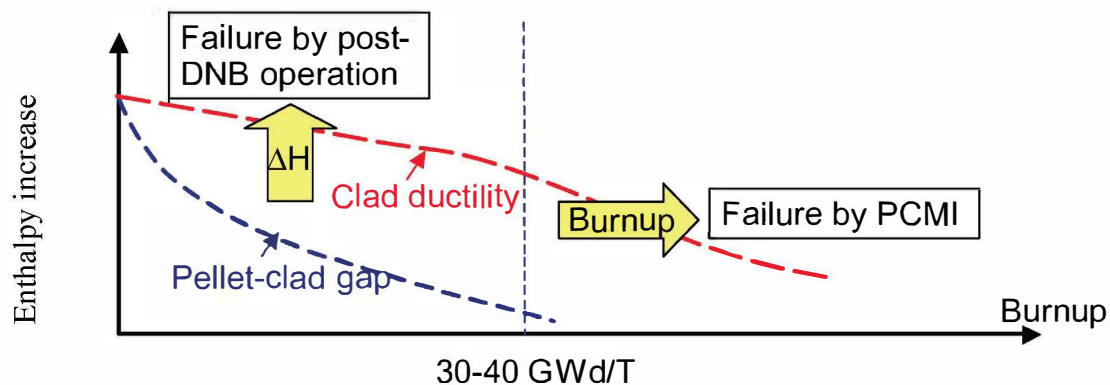


Figure 1-11: Cladding failure mechanisms, modified figure according to Montgomery et al., 2003.

The first record of *PCMI* failures may have been in *CANDU* fuel pins in the early to mid sixties, Cox, 2003. Although most of these failures started at massive hydride blisters on the tube *I.D.*, there were a small number that initiated at the outside and grew inwards. Typically the hydride in these pins was not enough to form the massive blisters, so the blisters progressively migrated to the *O.D.*, forming hydride lenses there, and leaving behind radial hydride. The cracks initiated at the outside and grew by fast fracture through the radial hydrides.

*PCMI* has never been reported to cause failures in either commercial *BWRs* or *PWRs*. However, there are some results generated in experimental reactors conducting ramp testing of heavily hydrided fuel claddings which indicate that massive hydride rims formed at the fuel cladding outer surface may cause crack formation at the cladding outer surface and crack propagation towards the inner cladding surface resulting in failures.

The ramp tests conducted in the Japanese Material Test Reactor indicated that rods irradiated for 3 cycles or less (corresponding to a burnup of 43 MWd/kgU) failed due to *PCI/SCC*, whereas at higher burnups, corresponding to irradiation for 4-5 cycles, there were some segments that failed by *PCMI*, see Section 3.3 for details.

A special case where *PCMI* failures may occur is during a Reactivity Initiated Accident, *RIA*. The reactivity transient during an *RIA* results in a rapid increase in fuel rod power leading to a nearly adiabatic heating of the fuel pellets and potentially *PCMI* fuel-cladding failures, see *ZIRAT 9 STR* on *LCA* and *RIA* for more details.

In a *PWR*, the most severe *RIA* scenario is the control rod ejection accident (*CREA*). The *CREA* is caused by mechanical failure of a control rod mechanism housing, such that the coolant pressure ejects a control rod assembly completely out of the core. The ejection and corresponding addition of reactivity to the core occurs within about 0.1 s in the worst possible scenario. With respect to reactivity addition, the most severe *CREA* would occur at hot zero power (*HZP*) conditions, i.e., at normal coolant temperature and pressure, but with nearly zero reactor power.

In a *BWR*, the most severe *RIA* scenario is the control rod drop accident (*CRDA*). The initiating event for the *CRDA* is the separation of a control rod blade from its drive mechanism. The separation takes place when the blade is fully inserted in the core, and the detached blade remains stuck in this position until it suddenly becomes loose and drops out of the core in a free fall.

Analyses of postulated *RIA* scenarios with state of the art three-dimensional neutron kinetics codes indicate that the width of the power pulse is in the range from 30 to 75 ms in fuel with burnup exceeding 40 MWdkg<sup>-1</sup>U<sup>-1</sup>, Meyer et al., 1997. Results also indicate that the power pulse in *BWRs* is longer than in *PWRs*, partly due to the fact that the mass of the *BWR* control rods is so much larger than that of the *PWR* control rod cluster.

*RIA* fuel performance may be tested in pulse reactors. The test conditions in these pulse reactors are much more severe than during a postulated *RIA* in a commercial reactor. Figure 1-12 shows an example of a *ZIRLO* rod tested in the Japanese *NSRR* pulse reactor. Base irradiation had occurred in the Ohi Unit 4 reactor, Fuketa et al., 2003. The *ZIRLO* rod failed at 120 cal/g, but the failure started at the location where the welded thermocouple was attached to the fuel cladding. Thus the failure could be an artefact due to the weld.



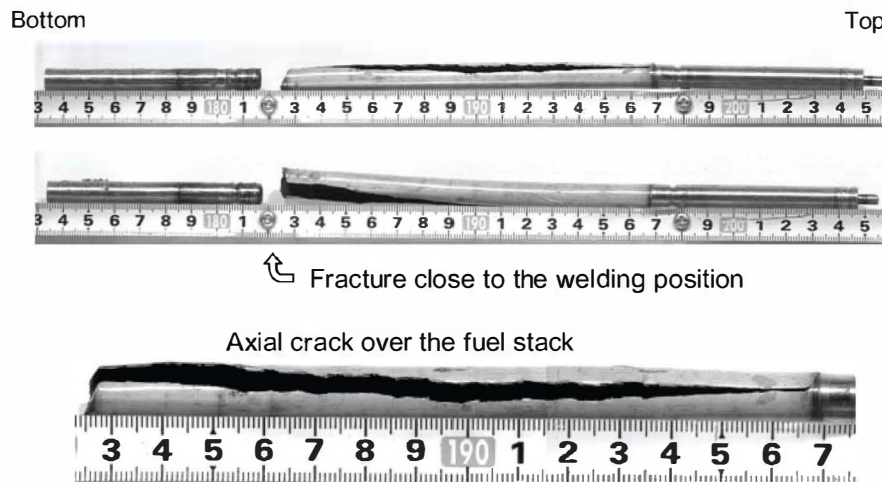


Figure 1-12: Test OI-11 (ZIRLO) Post-pulse rod appearance, Fuketa et al., 2003.

From other pulse reactor tests it has been shown that *PCMI* cracks may be initiated at the cladding outer surface due to the existence of a hydride rim reducing cladding ductility. Some of these incipient oxide cracks also propagate through the oxygen- and hydrogen-rich material just beneath the oxide. This subjacent material is also brittle, at least at room temperature, and the radial crack path through the oxide layer and the outer part of the cladding wall therefore appears characteristically brittle in fractographic examinations of high-burnup fuel rods, which have failed in *RIA* simulation tests, see e.g., the work by Fuketa et al., 2000 or Nakamura et al., 2002a. However, the radial crack path through the innermost part of the cladding wall generally indicates ductile failure, with the fracture surface typically inclined  $45^\circ$  to the main loading (hoop) direction. The ductile feature of the last part of the crack path is usually seen also in highly corroded and embrittled cladding, and it is believed that this inner ductile part of the cladding wall offers significantly higher resistance to the radial crack propagation than the brittle outer part. A typical crack path is shown in Figure 1-13.



Figure 1-13: Cladding failure initiated at a hydride blister in the CABRI REP Na-8 pulse reactor test, Papin et al., 2002.

There are essentially two different failure modes of the fuel rods dependant on burnup during an *RIA* see Figure 1-11.

**PCMI at high burnups** - The rapid increase in power leads to nearly adiabatic heating of the fuel pellets, which expand thermally and may cause fast straining of the surrounding cladding tube through pellet-cladding mechanical interaction. At this early heat-up stage of the *RIA*, the cladding-tube material is still at a fairly low temperature ( $<650$  K), and the fast straining imposed by the expanding fuel pellets may therefore cause a rapid and partially brittle mode of cladding failure, Chung & Kassner, 1998.

**Post-*dnb* at low burnups** - If the *RIA* transient is large enough, heat transferred from the pellets may bring the cladding outer surface to such a high temperature that dry-out or departure from nucleate boiling (*DNB*) occurs. If so, the cladding material could remain at a temperature above 1000-1200 K (resulting in rapid cladding oxidation) for up to 10 s, until rewetting takes place, Fuketa et al., 2001. For low burnup rods (with a small rod internal pressure and large pellet cladding gap), brittle fracture of the cladding material may occur during the re-wetting phase due to the abrupt quenching resulting in large thermal cladding stresses. This failure mode is imminent if the cladding tube is severely oxidized due to the *RIA* fuel cladding temperature excursion.

**PCI/PCMI Criteria** - During normal operation (class I) and anticipated operational occurrences (class II transients) there is no current criterion for fuel failure resulting from *PCI* according to the *NRC* Standard Review Plan, *SRP*<sup>3</sup>. Two related criteria should however be applied, but they are not sufficient to preclude *PCI* failures. These criteria are only valid for the fuel rods.

---

<sup>3</sup>NUREG-0800, 1981. *Standard review plan for the review of safety analysis reports for nuclear power plants, LWR edition, section 4.2: Fuel system design*, U.S. Nuclear Regulatory Commission report NUREG-0800, Rev. 2, Washington D.C.



- The transient induced uniform elastic and plastic strain should not exceed 1%. Since *PCI* failures may occur at lower strains than 1%, this criterion is not sufficient to ensure the non-occurrence of *PCI* failures.
- Fuel pellet melting should be avoided.

Normally, the smallest margin towards the 1% criterion is at about End of Cycle, *EOL* 1, when the fuel reactivity is largest (due to the effect of burnable absorbers). However, the smallest margin towards *PCI* failures (that may occur at strains less than 1%) occurs a burnup of about 35-40 MWd/KgU based upon ramp test results. Fuel rods may also potentially fail due to *PCMI* through the impact of hydrides that may decrease material ductility. The maximum amount of hydrides will occur at End of Life, *EOL* and consequently, the smallest margin towards *PCMI* failures are at *EOL*.

Acceptance criteria for fuel behaviour under *RIA* were established by the United States Nuclear Regulatory Commission (*USNRC*) in the late seventies, based on results from early *RIA* simulation tests in pulse reactor. These criteria have been used worldwide in their original or slightly modified forms. The original criteria are described next.

Firstly, a core coolability limit is defined, which states that the radial average fuel enthalpy may not exceed 280 cal/gUO<sub>2</sub> (1172 J/gUO<sub>2</sub>) at any axial location in any fuel rod. This limit is intended to ensure core coolability and reactor pressure vessel integrity by precluding violent expulsion of fuel particles into the coolant.

Secondly, a fuel rod failure threshold is defined, which states that cladding failure should be assumed in rods that experience radially averaged fuel enthalpies above 170 cal/gUO<sub>2</sub> (712 J/gUO<sub>2</sub>). This failure threshold is used in evaluations of radiological consequences of escaped fission products from failed rods, and it is not a definite operating limit. Hence, fuel enthalpies above this threshold are allowed in some of the fuel rods. It is noteworthy that in Germany, fuel failures during a *RIA* are not acceptable (even though the failures do not lead to fuel washout). The failure threshold is applicable to *RIA* events initiated from zero or low power, i.e. in practice to *BWR* *RIA* at *CZP* conditions. For *RIAs* occurring under rated power conditions, fuel rods that experience dry-out (*BWR*) or departure from nucleate boiling (*PWR*) should be assumed to fail.

**Parameters impacting *PCI/PCMI* fuel rod performance** are shown in Figure 1-14.

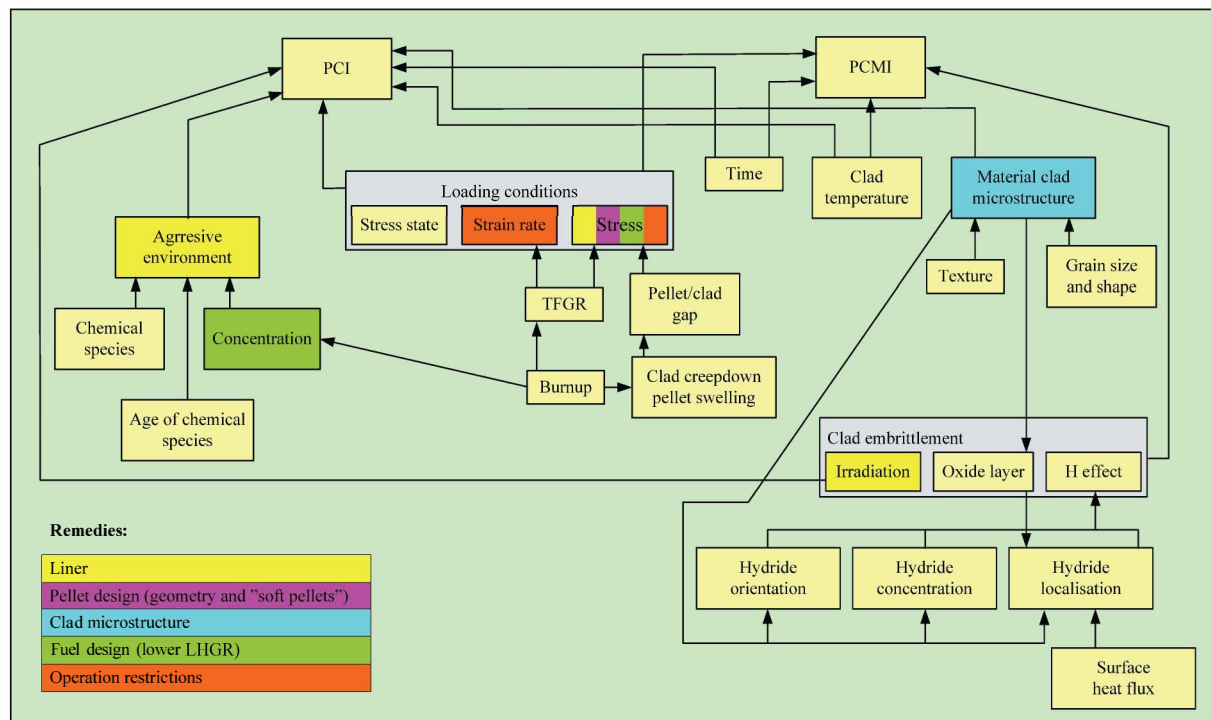


Figure 1-14: Parameters impacting *PCI/PCMI* performance.

## 1.1 PARAMETERS IMPACTING *PCI/PCMI*

### 1.1.1 Time

In ramp tests conducted in test reactors, the ramp rates are higher than those in commercial reactors. Higher ramp rates result in lower *PCI* thresholds since there is less time for stress relaxation. Thus, results obtained from ramp tests in test reactors tend to indicate a conservative *PCI* threshold. In the international ramp tests performed at Studsvik it was shown that a through-wall crack could be obtained in less than one minute, Figure 1-15 and, Figure 1-16. These figures also show that *RIA* transients are too short to be able to produce *PCI* cracks.

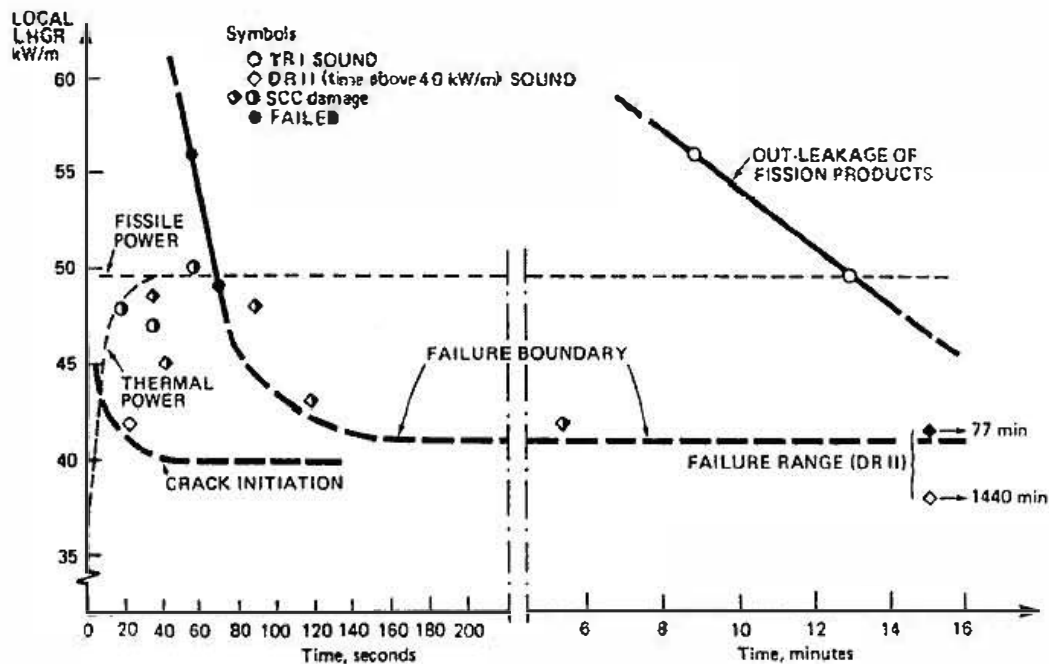


Figure 1-15: TRANS-RAMP I PCIF failure progression, BWR fuel, Mogard et al., 1988.

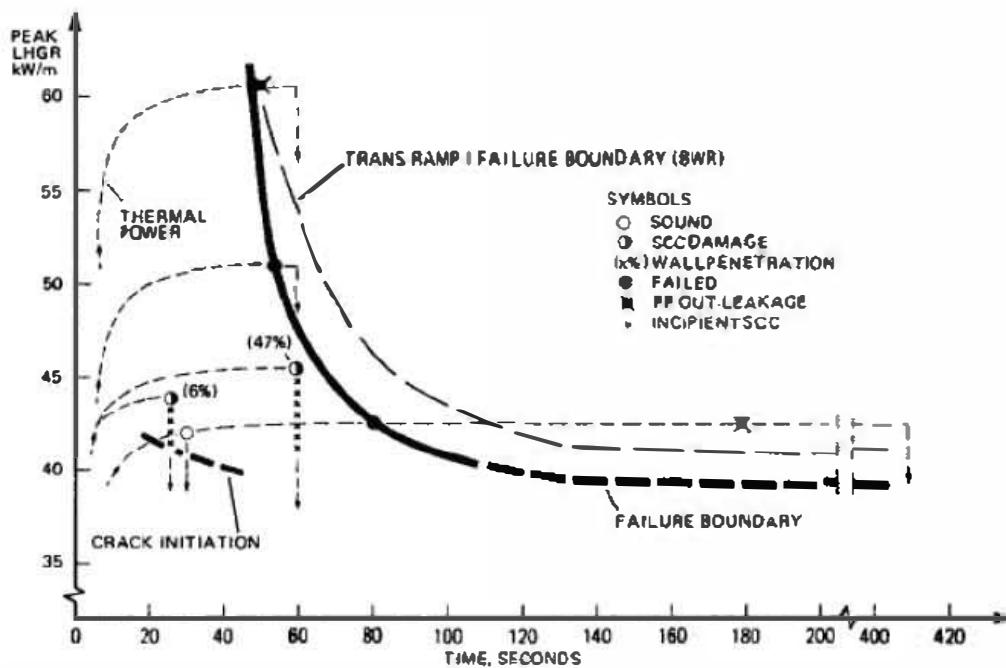


Figure 1-16: TRANS-RAMP II PCIF failure progression, PWR fuel, Mogard et al., 1988.

### 1.1.2 Aggressive environment

Figure 1-17 and Figure 1-18 shows the effect of Cs, Cd and Iodine on the SCC tendency of Zircaloy, see Section 2.1.2 for more details.

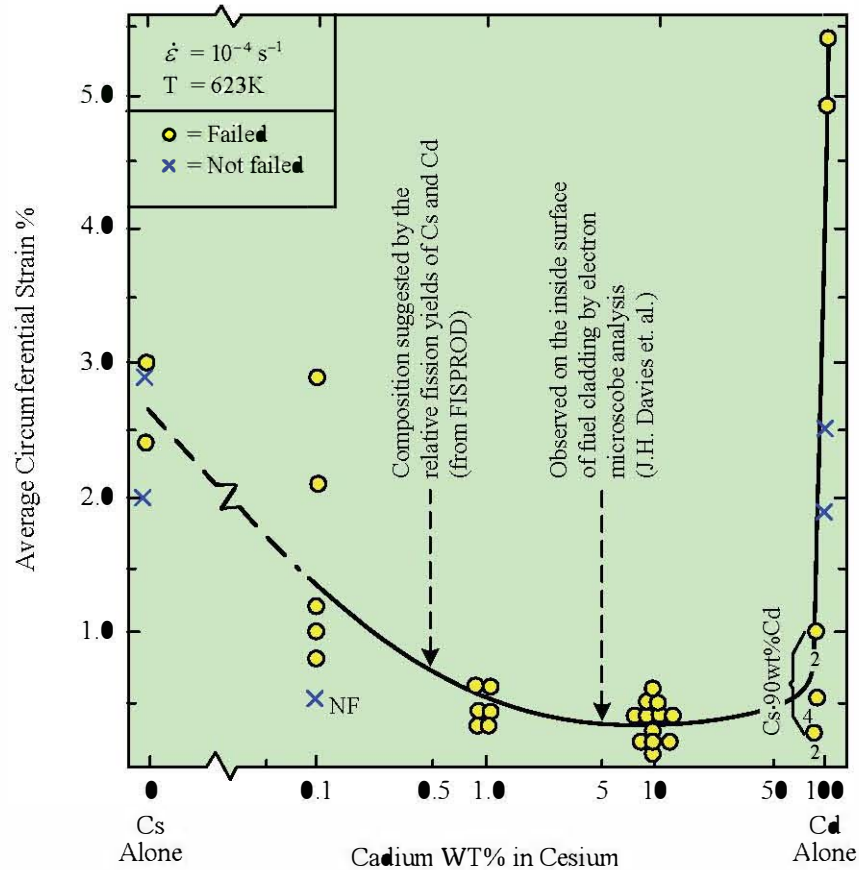


Figure 1-17: Average circumferential strain (%) versus composition of Cs-Cd corrodant (results from dynamic *SIMFEX* tests), modified figure according to Cox, 1990(b).

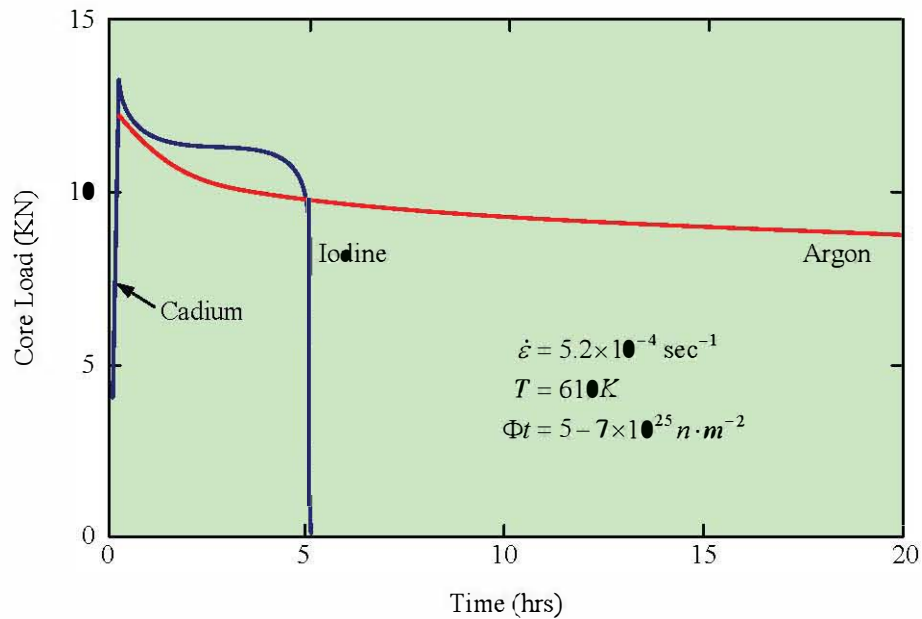


Figure 1-18: Core load (plane strain tests) versus time for ramp and hold, *RH*, expanding mandrel irradiated Zircaloy-2 tubes tested in argon, iodine (gas), and cadmium (liquid) at 610 K, modified figure according to Wisner & Adamson, 1982.

### 1.1.3 Cladding loading conditions

#### 1.1.3.1 Stress state

*PCI and PCMI* - Figure 1-19, Figure 1-20 and, Figure 1-21 shows that for similar hydrogen concentrations:

- The ductility varies in different tests and decreases in the order: uni-axial stresses > biaxial stresses with a stress ratio of  $\frac{\sigma_{\tan}}{\sigma_{axial}} = 2$  (burst test) -> biaxial stresses

with a stress ratio of  $\frac{\sigma_{\tan}}{\sigma_{axial}} = 1$  (*RIA* test). During the *RIA* test, the large friction

between the expanding pellet and the cladding will result in a ratio of  $\frac{\sigma_{\tan}}{\sigma_{axial}} = 1$ .

These results indicate that the stress state has a dramatic impact on cladding ductility. The implication of these results is that to obtain relevant data it is crucial that the stress state in an *RIA* simulation test is similar to that during an *RIA*, i.e.,

$$\frac{\sigma_{\tan}}{\sigma_{axial}} = 1.$$

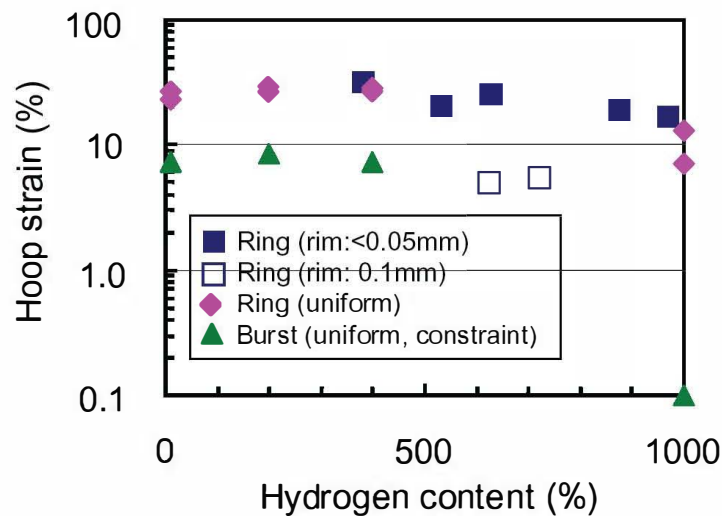


Figure 1-19: Cladding hoop strains at failure in ring tensile tests and residual hoop strains in burst tests of pre-hydrated *PWR* cladding, Nakamura et al., 2003(a).

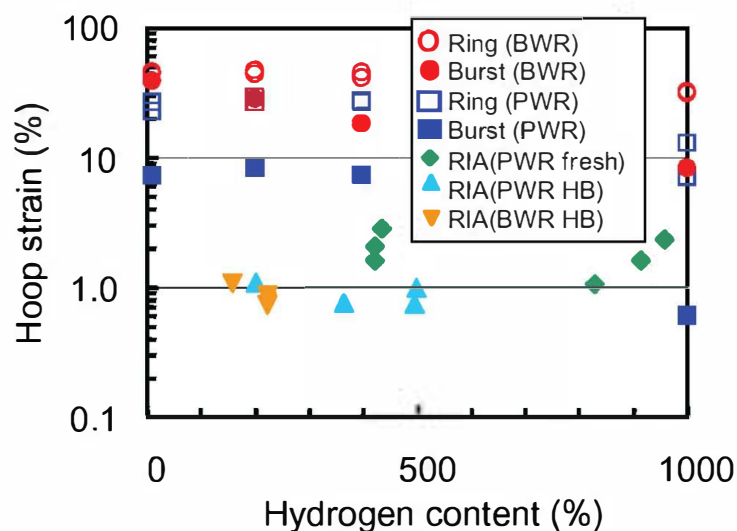


Figure 1-20: Comparison of failure hoop strains of fresh pre-hydrated *PWR* and *BWR* cladding in mechanical tests and in *RIA* tests. Failure strains of high burnup (*HB*) *PWR* and *BWR* fuels are plotted for comparison, Nakamura et al., 2003(a).

## 2 PCI DETAILS AND MODELS

### 2.1 PCI PHENOMENA

#### 2.1.1 General models and features (Ron Adamson)

Fuel-rod failures by pellet-cladding-interaction (*PCI*) occur during a power transient as a result of stresses developed by fuel-pellet expansion in the presence of an aggressive fission-product environment. The typical *PCI* cracks shown in Figure 2-1 are represented by schematic models in Figure 2-2, Figure 2-3 and Figure 2-4. Features of *PCI* cracking include:

- 1) usually occur after power ramping following significant exposure at low power
- 2) on the cladding outside surface the cracks characterized as “short and tight”, visually observed as pinholes or x-marks
- 3) observed plasticity is very small
- 4) metallographic examination usually reveals branching cracks and non-ductile fracture surfaces. In failed fuel the fracture surfaces are often obliterated by post-failure oxidation; however in cases where the crack surface is preserved, transgranular and intergranular fracture features such as in Figure 2-5 are observed. More fractography details are given in 2.1.3.

In failed fuel, the fracture surfaces are often obliterated by post-failure oxidation; however, in cases where the crack surface is preserved, transgranular and intergranular fracture features, such as in Figure 2-5, are observed.

Details of the cracking process, given in more depth in the Mechanism Section, 2.1.3, include:

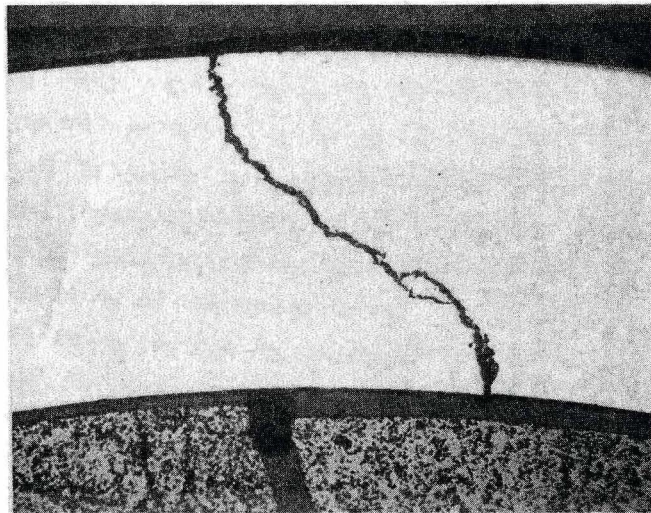
- Operation of the fuel rod for a time sufficient to generate substantial fission products, 5-10 MWd/Kg U.
- A power increase sufficient to
  - raise cladding hoop stress to near the yield stress,
  - increase in fuel temperature to allow release of fission products to the inner cladding surface. It is convenient for this to occur along a radial crack in the  $\text{UO}_2$  fuel, although it may also occur by migration of fission products to the pellet end followed by radial migration.
- A stress that remains “high” (although decreasing through creep relaxation of the cladding) to allow aggressive fission products to reach and penetrate inner-surface oxide. This occurs in minutes to tens of minutes.



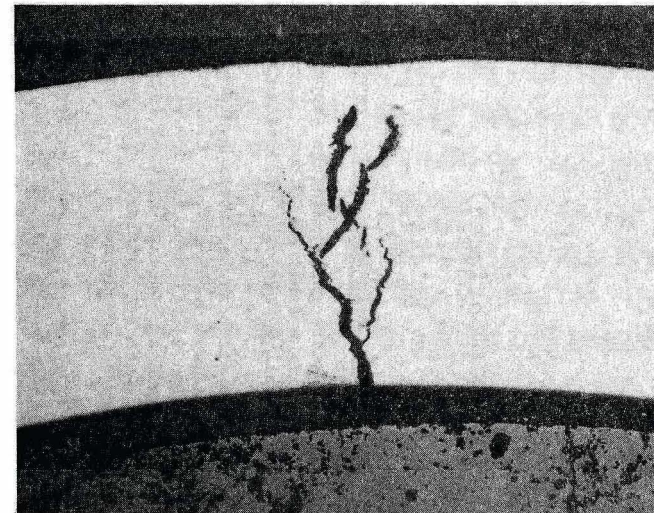
- Crack initiation on inner surface. Often this initiation is intergranular (particularly at low stress) but can also be transgranular cleavage combined with ductile tearing (fluting) at higher stresses.
- Crack propagation through the wall. Usually only one crack penetrates the wall, but multiple crack initiation can occur.
  - Through-wall penetration occurs quickly, in minutes.
  - the crack size is very small, such that as it reaches the surface it is a fine pinhole, on the order of 25  $\mu\text{m}$  (.001 inch) in “diameter”.
- Ending of the stress-corrosion cracking process, as exposure of the crack to steam shuts off the *SCC* reaction. This is certainly true for iodine-based reactions, and is less certain for Cd based reactions.
  - steam flows through the crack and enters the rod interior
  - the crack surface is oxidized, sometimes to the extent that the pinhole opening is closed by the oxide.
- Crack extension in the axial direction
  - for relatively low stresses, a short crack, 25-50  $\mu\text{m}$  (1-2 mils), could form. It would look like >---< , a brittle straight crack with ductile shear lips at its ends (the “x-mark”).
  - at higher stresses, further extension in the axial direction might occur. However, since very little hydriding occurs at this location the *PCI* crack, the primary crack, is usually not the source of long split “secondary cracks”.

The *PCI* models of Figure 2-3 and Figure 2-4 illustrate important features; however the “eventual ductile fracture” designated in Figure 2-4 is exaggerated, as such ductility is usually restricted to highly local deformation at the cladding surface which results in the characteristic x-marks of Figure 2-6.





0601.02



0607.02

Figure 2-1: *PCI* cracks in Zircaloy-2 fuel rods, Davies et al., 1984.

### 3 PELLET-CLADDING MECHANICAL INTERACTION (PCMI) (RON ADAMSON)

Many aspects of *PCMI* loading are the same as for *PCI*. However, *PCMI* failures do not occur by stress-corrosion cracking and therefore do not involve attack by fission products. The most important environmental factor is frequently the presence of hydrides.

#### 3.1 EFFECTS OF HYDRIDES

As background for *PCMI*-type failures, a brief summary of hydride effects is given here. All zirconium alloy reactor components absorb hydrogen during reactor service through the corrosion reaction between zirconium and water. Basics of these phenomena are given in ZIRAT Special Topical Report “Hydriding Mechanisms and Impact on Fuel Performance”, Cox & Rudling, 2000, and are reviewed in all of the ZIRAT Annual Reports. Hydrides tend to embrittle zirconium alloys and therefore their effects are important for in-reactor normal service, for ex-reactor handling operations and for accident and transient scenarios such as *LOCA* and *RIA*. It is unclear whether individual hydrides themselves are actually brittle at all normal reactor temperatures, Shi & Puls, 1999, or become ductile at about 300°C (573 K), Cox & Rudling, 2000 and Yagnik et al., 2004(b); however it is clear that high concentrations of hydrides (5000-16000 ppm) are very brittle, as in hydride blisters or rims.

Under normal conditions, hydride platelets form in the circumferential direction in fuel cladding, as illustrated in Figure 3-1(a). Under some circumstances such as during long-term storage or during power transients, they can form in the radial direction, Figure 3-1(b). Because in high-power rods a temperature gradient encourages hydrogen to diffuse to the colder outer cladding surface, rims of hydrides can form, as illustrated in Figure 3-2.

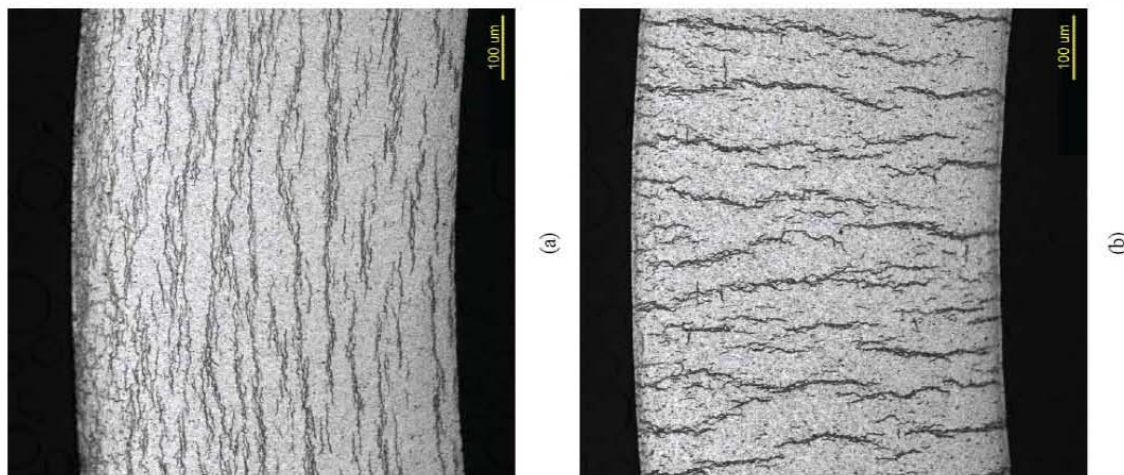


Figure 3-1: Hydride orientation in Zircaloy-4 (SR4) cladding. a) circumferential, b) radial, Chu et al., 2005.

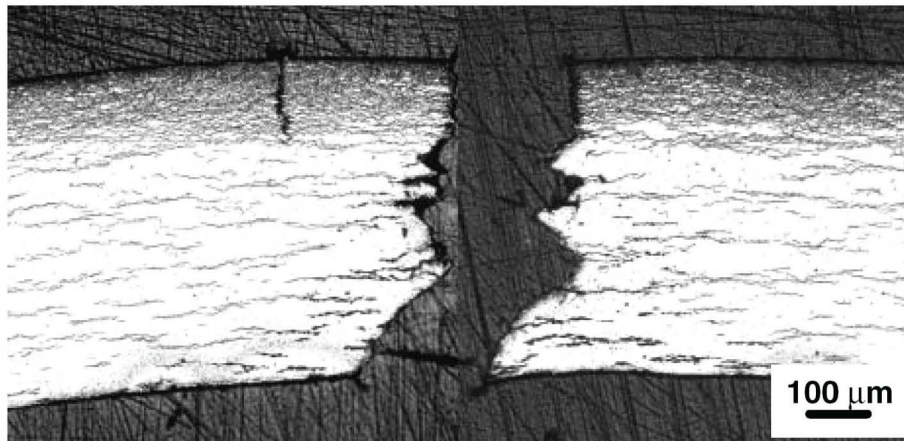


Figure 3-2: Hydride rim and associated cracks in cladding failed in a room temperature burst test, Nagase & Fuketa, 2005.

Hydrides effects are listed here, giving appropriate figures and references.

- 1) The effect of hydrides is strongly dependent upon testing temperature. Material at 300°C (573 K) (reactor operating temperature regime) retains much more ductility (uniform elongation, *UE*; total elongation, *TE*; reduction in area, *RA*) than at 20°C (293 K) (handling temperature regime); see Figure 3-2(a), Figure 3-2(b), Figure 3-5, Figure 3-6, Figure 3-7, Figure 3-8 and Figure 3-9.



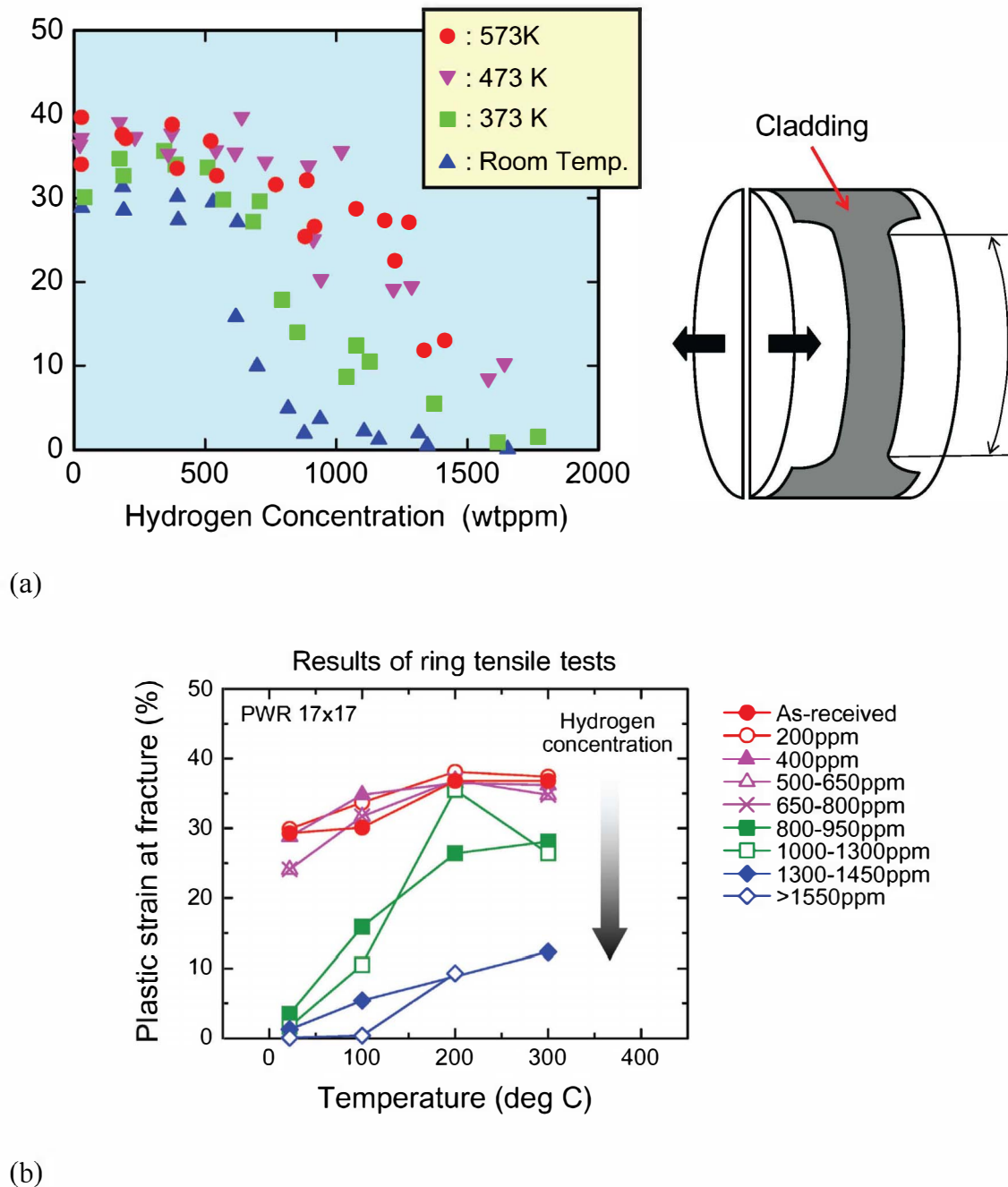


Figure 3-3: (a) Failure Strain as a function of Hydrogen Concentration of ring tensile-test samples, (b) Temperature effect on cladding ductility, Fuketa et al., 2003.

## 4 SUMMARY

### 4.1 OVERALL – SECTION 1

Stresses which induce both *PCI* and *PCMI* are caused by expansion of the fuel pellet against the cladding during power increases. *PCI* failures are driven by fission product release from the fuel, while *PCMI* failures are usually driven by mechanical cracking, often enhanced by local hydrides.

Increased burnup will reduce the pellet-cladding gap prior to the ramp, and may therefore decrease both the *PCI* and *PCMI* threshold.

Several burnup dependent parameters may impact *PCI/PCMI* performance. More data at higher burnups are needed to assess the burnup effect on *PCI/PCMI* threshold

*PCI/PCMI* margins may be reduced at higher burnups due to:

- More fission products (I, Cs and Cd) produced.
- Increased Transient Fission Gas Release, *TFGR*.
- Development of a hydride rim at the cladding outer surface, more radial hydrides (that may promote *PCMI* failures).

*PCI/PCMI* margins may be increased at higher burnups due to:

- Formation of pellet peripheral radial cracks that may reduce stress concentrations in the claddings during *PCI/PCMI* loadings
- Increased pellet-cladding creep rates (making the pellets “softer”)

It is unclear how the following microstructural changes may impact *PCI/PCMI* performance

- Fuel-cladding bonding and formation of a porous pellet rim zone at fuel pellet average burnup of about 50 MWd/kgU.

In general the *PCI/PCMI* margins may be increased by:

- Ramp testing and hot-cell *PIE* of high burnup fuel, i.e., research/development/performance evaluations.
- Using low *LHGR* fuel designs.

- Using liner/barrier claddings (it is noteworthy that liner/barrier claddings do not totally eliminate the *PCI* failures but increases the margins towards these types of failure. *PCI* failure is a statistical phenomena which means that even with liner/barrier fuel *PCI* failures may occur at fairly low *LHGR*, even though the probability of failure is low.
- Evaluation of the relevance of the fuel vendor operating restrictions. Best *PCI* margins are of course obtained if liner/barrier fuel is used together with the operating restrictions for non-barrier fuel.
- Getting away from control cells and back to scatter loading.
- Using fuel claddings with high corrosion and hydride resistance (thus reducing the hydrogen pickup in the cladding).
- Increased understanding of the effects of hydrides and hydride distribution on crack initiation and propagation.
- Using pellets that are “soft” and with large grains.
- Control of pellet manufacturing parameters resulting in higher integrity pellets (avoiding pellet defects).

#### 4.2 *PCI PHENOMENA – SECTION 2.1*

Pellet-cladding-interaction (*PCI*) fuel rod failures occur during a power transient as a result of stresses developed by fuel pellet expansion in the presence of an aggressive fission-product environment. Features of *PCI* cracking include:

- usually occur after power ramping following significant exposure at low power
- on the cladding outside surface the cracks characterized as “short and tight”, visually observed as pinholes or x-marks
- observed plasticity is very small
- metallographic exam usually reveals branching cracks and non-ductile fracture surfaces. In failed fuel the fracture surfaces are often obliterated by post-failure oxidation; however in cases where the crack surface is preserved, transgranular and intergranular fracture features are observed.

Irregularities of the pellet surface, such as a missing portion or a chip, can significantly enhance the failure probability.

Careful and expert interpretation of post-failure metallography is required to obtain a true understanding of the failure details.

In-reactor ramp test techniques have been developed which produce reliable fuel rod performance insights.

In general, laboratory testing using unirradiated or, especially, irradiated zirconium alloys, are useful in addressing a problem in that it can:

- EXPLAIN qualitative details: what is going on?; can a model be developed?
- SIMULATE the phenomena: what are the major metallurgical and mechanical issues?
- FIX the problem: what might work?; which fixes are best or most practical?

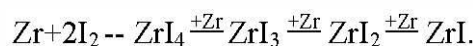
When attempting to simulate *PCI* conditions it is important to:

- use appropriate stress and strain states
- provide the appropriate strain and strain concentrations
- use appropriate chemistry conditions (for I, Cs, Cd)
- avoid extraneous chemistry effects, such as the reactions of I with Fe or water vapour.

A good data base exists in the open literature reporting “*PCI* testing” using ring specimens, localized ductility specimens, internally pressurized tubes and expanding mandrels.

The *PCI* mechanism may be summarised as follows:

- a. *PCI* cracking is a form of *SCC* caused by fission products (FP) released from the  $\text{UO}_2$  by an increase in local power density. The most probable fission product involved is iodine, but Cs/Cd mixtures cannot be eliminated on present evidence.
- b. Iodine released from the fuel reacts with the Zircaloy *I.D.* surface at sites where the protective oxide has been cracked. A series of iodides is formed:



Of these iodides,  $\text{ZrI}_4$  is the most aggressive iodide, and is far more aggressive than  $\text{I}_2$ ;  $\text{ZrI}_2$  and  $\text{ZrI}$  have low volatility and are incapable of causing *SCC* cracking.

- c. At the start of a power ramp, (if there has been no prior release of iodine) the  $\text{I}_2$  released in the ramp will react with the Zr surface exposed at cracks in the oxide causing *IG* attack and forming  $\text{ZrI}_4$ . The extent of *IG* attack will be determined by the time it takes to generate enough  $\text{ZrI}_4$  to permit *TG* crack propagation.

## 5 REFERENCES

Ainscough J. B., Rigby F. and Osborn S. C., “*The effect of titania on grain growth and densification of sintered  $UO_2$* ”, J. Nucl. Materials, 52, pp 191 1974.

Ainscough J. B., Rigby F. and Morrow S. A., “*Effect of oxygen potential on the thermal creep of niobia doped  $UO_2$* ”, Journal of the American Ceramic Society, Vol. 64, Issue 5, pp 315, 1981.

Aitchison I. and Cox B., “*Interpretation of Fractographs of SCC in Hexagonal Metals*”, Corrosion, v.28, pp 83 – 87, 1972.

Adamson R. B., “*Effect of Texture on Stress Corrosion Cracking of Irradiated Zircaloy in Iodine*”, J. Nucl. Mat. 82, pp. 363, 1980.

Adamson R. B. and Bell W. L., “*Effects of Neutron Irradiation and Oxygen Content on the Microstructure and Mechanical Properties of Zircaloy*”, Microstructure and Mechanical Behavior of Materials, Proceedings of the International Symposiums, Xian, China, Oct. 1985, EMAS, Warley, UK, pp. 237-246, 1985.

Adamson R. B., Wisner S. B., Tucker R. P., and Rand R. A., “*Failure Strain for Irradiated Zircaloy Based on Subsize Specimen Testing and Analysis*”, The Use of Small-Scale Specimens for Testing Irradiated Material, ASTM STP 888, W. R. Corwin and G. E. Lucas, Eds., American Society for Testing and Materials, pp. 171-185, 1986.

Adamson R. B., “*Effects of Neutron Irradiation on Microstructure and Properties of Zircaloy*”, Zirconium in the Nuclear Industry, ASTM STP 1354, American Society for Testing and Materials, pp. 15-31, 2000.

Adamson R. B. and Rudling P., “*Mechanical Properties of Zirconium Alloys*”, ZIRAT-6 Special Topical Report, 2001.

Andersson T. and Wilson A., “*Ductility of Zircaloy Canning Tubes in Relation to Stress Ratio in Biaxial Testing*”, Zirconium in the Nuclear Industry, ASTM STP 681, American Society for Testing and Materials, pp. 60-71, 1979.

Andersson T., Almberger J and Björnkvist L., “*A Decade of Assembly Bow Management at Ringhals*”, ANS Topical Meeting on Light Water Reactor Fuel Performance, Orlando, Fl., 2004.

Arborelius J., Backman K., Hallstadius L., Limback M., Nilsson J., Rebensdorff B., Zhou G., Kitano K., Lofstrom R. and Ronnberg G., “*Advanced doped  $UO_2$  pellets in LWR applications*”, Paper # 1099, Track# 1, 2005 Water Reactor Fuel Performance Meeting, 2-6 October, Kyoto, 2005.

Armijo J. S., *Performance of Failed BWR Fuel*. Proceeding from Light-Water-Reactor-Fuel-Performance, West Palm Beach, Fl., pp 410-422, April 17-21, 1994.



Armijo J. S., Coffin L. F. and Rosenbaum H. S., “*Development of Zirconium Barrier Fuel Cladding*”, Proc. 10<sup>th</sup> Int. Symp. on Zr in the Nucl. Ind., ASTM-STP-1245, pp. 3-18, Baltimore, MD, 1994.

Arsene S. and Bai J. B., “*A new approach to measuring transverse properties of structural tubing by a ring test*”, Laboratory MSS/MAT, Ecole Centrale Paris, CNRS URA 850, 92295 Chatenay Malabry Cedex, France 1996.

Arsene S., Bai J. B. and Bompard P., “*Hydride Embrittlement and Irradiation Effects on the Hoop Mechanical Properties of Pressurized Water Reactor (PWR) and Boiling-Water Reactor (BWR) ZIRCALOY Cladding Tubes: Part I. Hydride Embrittlement in Stress-Relieved, Annealed, and Recrystallized ZIRCALOYs at 20°C and 300°C*”, Metallurgical and Materials Transactions A Volume 34A, pp. 553-566, March 2003.

Assman H., Doerr W., Gradel G. and Peechs M., “*Doping UO<sub>2</sub> with niobia – Beneficial or not?*”, J. Nucl. Materials, 98, pp 216, 1981.

Baily W. E. et al, Proc. ANS Top. Meeting LWR Fuel Performance, p. 26-35, Avignon, France, Apr. 21-24, 1991.

Balourdet M., Bernaudat C., Basini V. and Hourdequin N., “*The PROMETRA Programme: Assessment of Mechanical Properties of Zircaloy 4 Fuel Properties During an RIA*”, Transactions of the 15<sup>th</sup> International Conference on Structural Mechanics in Reactor Technology (SMIRT-15), pp. II-485-492, Seoul, Korea, August 15-20, 1999.

Barrio F. J. and Herranz L. E., “*Predictive methodology of a cladding failure criterion based on PROMETRA database: Application to CABRI-CIP01 experiment*”, Proc. EHPG Meeting, Gol, OECD Halden Reactor Project Report HPR-359, ‘Volume 2, Halden, Norway, September 8-13, 2002.

Bates D. W., Koss D. A., Motta A. T. and Majumdar S., “*Influence of Specimen Design on the Deformation and Fracture of Zircaloy Cladding*”, Proceedings of the ANS Int. Topical Mtg. on LWR Fuel Performance, American Nuclear Society, pp. 1201-1210, Park City, UT, 2000.

Billaux M. and Moon H., “*Pellet-Cladding Mechanical Interaction In Boiling Water Reactors*”, NEA/OECD Seminar on Pellet-Clad Interaction in Water Reactor Fuels, Aix-en-Provence, 2004.

Blomberg G., “*Results of recent Hot Cell examinations of failed fuel at Studsvik, Sweden*” 35<sup>th</sup> International Utility Nuclear Fuel Performance Conference, 2006.

Bourgeois L., Dehaut Ph., Lemaignan C. and Hammou A., “*Factors governing microstructure development of Cr<sub>2</sub>O<sub>3</sub>-doped UO<sub>2</sub> during sintering*”, Journal of Nuclear Materials, 297 pp 313, 2001.

Busby C. C., Tucker R. P., and McCauley J. E., J. Nucl. Mat. 55, pp. 64, 1975; and in Bettis Atomic Power Laboratory Report WAPD-TM1149, 1974.

Cheadle B. A., Ells C. E., and van der Kuur J., “*Plastic Instability in Irradiated Zr-Sn and Zr-Nb Alloys*”, Zirconium in Nuclear Applications, ASTM STP 551, American Society for Testing and Materials, pp. 370-384, 1974.

Chu H. C., Wu S. K., Kuo R. C. and Cheng S. C., “*Effect of Radial Hydrides on Mechanical Properties of Zircaloy-4 Cladding*”, Proc. Water Reactor Fuel Performance Meeting, Kyoto, Japan, October 2-6, 2005.

Chung H. M. and Kassner T. F., 1998.

Coffin L., Zirconium in the Nuclear Industry, ASTM STP 681, American Society for Testing and Materials, pp. 72, 1978; and in Proceedings of the ANS Topical Meeting on Water Reactor Fuel Performance, St. Charles, IL, pp. 346, 1977.

Coleman C. E., Proceedings of the Conference on Physical Metallurgy of Reactor Fuel Elements, Berkeley, UK, (Metals Society, London), pp. 302, 1973.

Coleman C. E. and Cox B., “*Cracking Zirconium Alloys in Hydrogen*”, Zirconium in the Nuclear Industry: Sixth International Symposium, ASTM STP 824, D. G. Franklin and R. B. Adamson, Eds. American Society for Testing and Materials, pp. 675-690, 1984.

Coleman C. E., “*Simulating the Behavior of Zirconium-Alloy Components in Nuclear Reactors*”, Zirconium in the Nuclear Industry, ASTM STP 1423, American Society for Testing and Materials, 2002.

Cox B., “*Stress Corrosion Cracking of Zircalloys in Iodine Containing Environments*”, Proc. Conf. On Zr in Nuclear Applications, Portland, OR, Aug, 1973, ASTM-STP-551, pp 419 – 434, 1974.

Cox B and Wood J. C., “*Corrosion Problems in Energy Conversion and Generation*”, ed. By Craig S., Tedman Jr., Electrochem. Soc., p. 275. New York, 1974.

Cox B., “*Environmentally-Induced Cracking of Zirconium Alloys – A Review*”, Revs. On Coatings and Corrosion, Freund, Tel Aviv, v.4, #2, pp 367 - 422, 1975.

Cox B. and Wood J. C., “*The Mechanism of SCC of Zirconium Alloys in Halogens*”, Proc. Int. Conf. On Mechanisms of Environment Sensitive Cracking of Materials, University of Surrey, Guildford, Metals Soc., London, U.K., 1977.

Cox B. and Haddad R., J. Nucl. Mat. 137, pp. 115, 1986.

Cox B., “*Stress Corrosion Cracking of Zirconium Alloys*”, Lanmuir, v.3, pp 867 – 873, 1987.